Physica E 85 (2017) 65–73

Contents lists available at ScienceDirect

Physica E

journal homepage: www.elsevier.com/locate/physe

Electronic properties and STM images of vacancy clusters and chains in functionalized silicene and germanene

Pooja Jamdagni [a,*], Ashok Kumar [b], Munish Sharma [a], Anil Thakur [c,*], P.K. Ahluwalia [a,*]

[a] Department of Physics, Himachal Pradesh University, Shimla, HP 171005, India
[b] Centre for Physical Sciences, School of Basic and Applied Sciences, Central University of Punjab, Bathinda 151001, India
[c] Department of Physics, Govt. P.G. College, Solan, HP 173212, India

HIGHLIGHTS

- Hexagonal & rectangle vacancy clusters retain the semiconducting nature of monolayers.
- Pentagonal and triangle vacancy clusters introduce metallicity and magnetic character.
- Vacancy chain patterns induce small bandgap in O-functionalized monolayers.
- STM images show distinctly different characteristics for various vacancy patterns.
- STM images can be used as electronic fingerprints to identify vacancy patterns created during functionalization.

ARTICLE INFO

Article history:
Received 16 April 2016
Received in revised form
1 July 2016
Accepted 12 August 2016
Available online 12 August 2016

Keywords:
DFT
Silicene
Germanene
Electronic structure
STM
Functionalization

ABSTRACT

Electronic properties and STM topographical images of X (=F, H, O) functionalized silicene and germanene have been investigated by introducing various kind of vacancy clusters and chain patterns in monolayers within density functional theory (DFT) framework. The relative ease of formation of vacancy clusters and chain patterns is found to be energetically most favorable in hydrogenated silicene and germanene. F- and H-functionalized silicene and germanene are direct bandgap semiconducting with bandgap ranging between 0.1–1.9 eV, while O-functionalized monolayers are metallic in nature. By introducing various vacancy clusters and chain patterns in both silicene and germanene, the electronic and magnetic properties get modified in significant manner e.g. F- and H-functionalized silicene and germanene with hexagonal and rectangle vacancy clusters are non-magnetic semiconductors with modified bandgap values while pentagonal and triangle vacancy clusters induce metallicity and magnetic character in monolayers; hexagonal vacancy chain patterns induce direct-to-indirect gap transition while zigzag vacancy chain patterns retain direct bandgap nature of monolayers. Calculated STM topographical images show distinctly different characteristics for various type of vacancy clusters and chain patterns which may be used as electronic fingerprints to identify various vacancy patterns in silicene and germanene created during the process of functionalization.

1. Introduction

Silicene and germanene, the silicon and germanium equivalent of atomic layer of Carbon (graphene), have recently attracted a significant attention [1–5] due to their similar electronic properties as exhibited by graphene [6–8]. Theoretical studies [7,8] have predicted the stability of both silicene and germanene in buckled two-dimensional (2D) honeycomb structure. The buckling is due to the mixture of sp^2 and sp^3 hybridization. The realization of freestanding silicene and germanene are still challenging for the experimentalists, however, experiments have shown that silicene and germanene can be grown on metal substrates such as Ag(111) [9–11], Au(111) [12], Ir(111) [13], etc.. The experimental realization of monoatomic layers of Si and Ge in free-standing form may be expected in the near future.

The presence of Dirac cone in atomic layers of group-IV elements including silicene and germanene allows continuous conduction near the Fermi level which limits their direct application in electronic devices. Consequently, alternative techniques such as covalent functionalization have been opted to modify the physical, chemical and electronic properties of 2D monoatomic layers e.g.

* Corresponding authors.
E-mail addresses: j.poojaa1228@gmail.com (P. Jamdagni), anilt2001t@gmail.com (A. Thakur), pk_ahluwalia7@yahoo.com (P.K. Ahluwalia).

http://dx.doi.org/10.1016/j.physe.2016.08.015
1386-9477/

hydrogenated graphene can serve as natural host for graphene quantum dots, cluster of vacancies in hydrogen sublattice [14]; energy gap opens up in SiGe-based 2D layered structures on hydrogenation [15] which can be further modified by external electric field and in-plain strains [15–17]; single hydrogen and hydroxyl vacancies on siloxene (H and OH functionalized silicene) induce spin-polarization in the 2D lattice [18]; hydrogen terminated silicene and germanene nanoribbons show half metallicity which offers their use in spintronics applications [19]; hydrogen passivation of the zigzag edges of hybrid graphene/h-BN nanoribbons provides mechanical strength and stability to 1D superlattice [20] etc.

Not only hydrogenation, but the covalent functionalization of layered structures with halogens and oxygen is also possible. It is well known fact that the hydrogenation and fluorination processes provide structures that are energetically accessible and easy to synthesize in the laboratory [21,22]. Hydrogen and fluorine derivatives of silicene and germanene are known to be semiconducting with a bandgap ranging from 0.2 eV to 2.0 eV [23,24] whereas oxygen derivative of silicene and germanene may be metallic, semiconducting or insulating depending upon the oxidation conditions [25–27].

However, in the process of functionalization and physical or chemical desorption, it is always possible that a small amount of vacancies may get created. Also, it is possible to do full, partial or site specific functionalization of nanomaterials along with the creation of vacancies through lithography technique. The hydrogenation of silicene on Ag(111) substrate at room temperature results into perfectly ordered superstructure, however, dehydrogenation occurs on annealing at moderate temperature [28]. Similarly, partially hydrogenated phase has been found to produced in the process of hydrogenation of silicene [29]. In addition, functionalization and vacancies in nanomaterials induce magnetism [30–32], which has potential applications in the fast emerging field of nanoelectronics and spintronics.

The above possibilities of the occurrence of vacancies in the experiments and their potential applications triggered our interest to explore what role vacancies may play in hydrogenated, fluorinated and oxidized silicene and germanene? In this paper, the electronic and magnetic properties along with the STM topographical images of various vacancy patterns in functionalized silicene and germanene are systematically investigated.

2. Computational method

Calculations have been performed by using SIESTA simulation package [33]. Norm conserving Troullier Martin pseudo-potential in fully separable Kleinman and Bylander form have been used to treat the electron-ion interactions [34]. The exchange and correlation energies have been treated within the General Gradient Approximation (GGA) according to the Perdew–Burke–Ernzerhof (PBE) parameterization. The Kohn Sham orbital's were expanded in a linear combination of numerical pseudo atomic orbital's using a split-valence double zeta basis set with polarization functions (DZP). Throughout geometry optimization confinement energy of numerical pseudo-atomic orbital's are taken as 0.01 Ry. Minimization of energy was carried out using standard conjugate-gradient (CG) technique. Structures were relaxed until the forces on each atom were less than 0.01 eV/Å. A $30 \times 30 \times 1$ Monkhorst pack of k-point was used for sampling the Brillion zone. The spacing of the real space used to calculate the Hartree exchange and correlation contribution of the total energy and Hamiltonian was 250 Ry. A 4×4 supercell with a vacuum of about 20 Å along perpendicular to 2D plane has been used in our calculations.

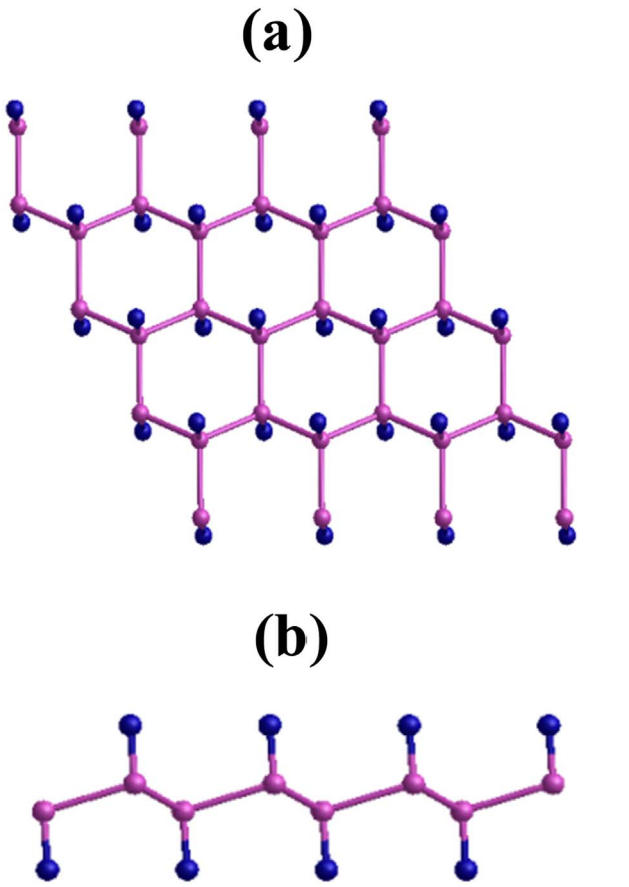

Fig. 1. (a) Top and (b) side view of functionalized silicene or germanene. Violet color balls represents Si or Ge atoms whereas blue color balls represents X atoms, where X=F or H or O. (For interpretation of the references to color in this figure legend, the reader is referred to the web version of this article).

3. Results and discussions

Fig. 1(a) and (b) depict the top and side view of X (=F, H, O) functionalized silicene and germanene. Well known mixed sp^2 and sp^3 hybridization in silicene and germanene provides a favorable platform for their functionalization. A fully relaxed 4×4 supercell of 64 atoms of Si or Ge and F or H or O in chair configuration has been taken as a unit cell in the study. Note that chair-configuration of functionalized silicene and germanene is most stable [15] where X atoms on Si or Ge are at alternating above and below positions (Fig. 1(b)). Various vacancy clusters are introduced in functionalized silicene and germanene by removing X (=F, H, O) atoms (Fig. 2). For example, hexagonal vacancy cluster can be created by removing six adjacent X-atoms of functionalized monolayer (Fig. 2 (a)). Similarly, removing of five, four and three atoms results into pentagonal, rectangle and triangle vacancy cluster respectively (Fig. 2(b)–(d)). These different shape vacancies confine 6, 5, 4, and 3 electrons respectively in the vacancy forming region. The various alternating vacancy chains in functionalized silicene and germanene have been created by removing whole row of hexagonal, rectangle and zigzag pattern of periodic supercell (Fig. 3).

Electronic band structure calculations show fluorine and hydrogen functionalized silicene and germanene to be a semiconductor whereas oxygen functionalized silicene and germanene are metallic in nature (Fig. 4). The bandgap values of SiF, SiH, GeF and GeH are found to be as 0.81 eV, 1.92 eV, 0.12 eV and 0.94 eV respectively. It is found that valance band maximum (VBM) and conduction band minimum (CBM) lies on Γ high symmetry point that makes these functionalized monolayers as direct bandgap

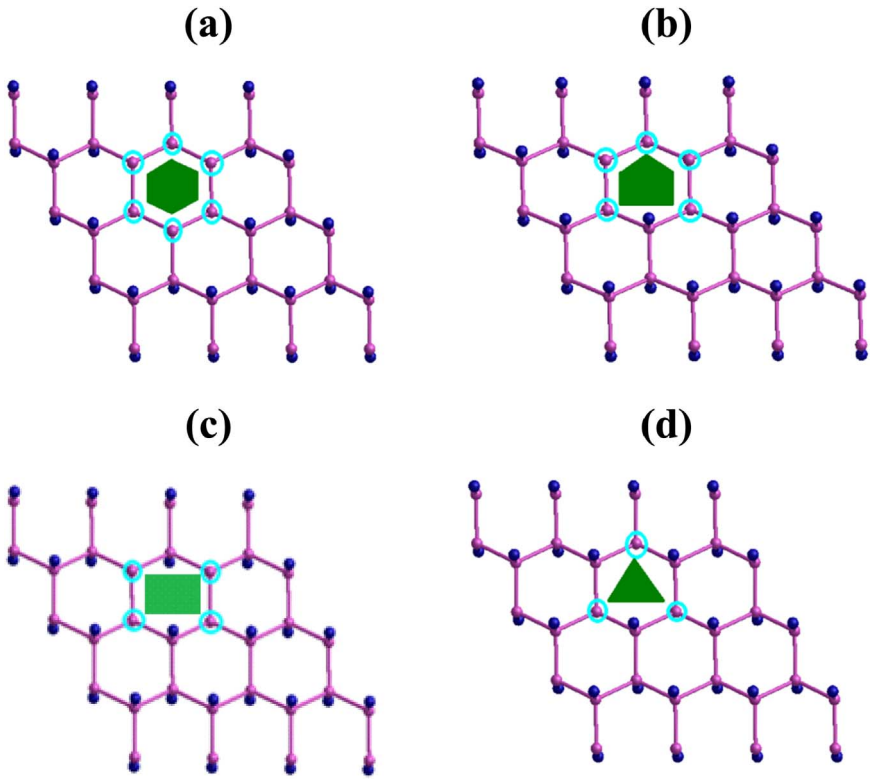

Fig. 2. Various vacancy clusters (a) hexagonal, (b) pentagonal (c) rectangle and (d) triangle formed by removing six, five, four and three X (=F, H, O) atoms respectively from functionalized silicene and germanene.

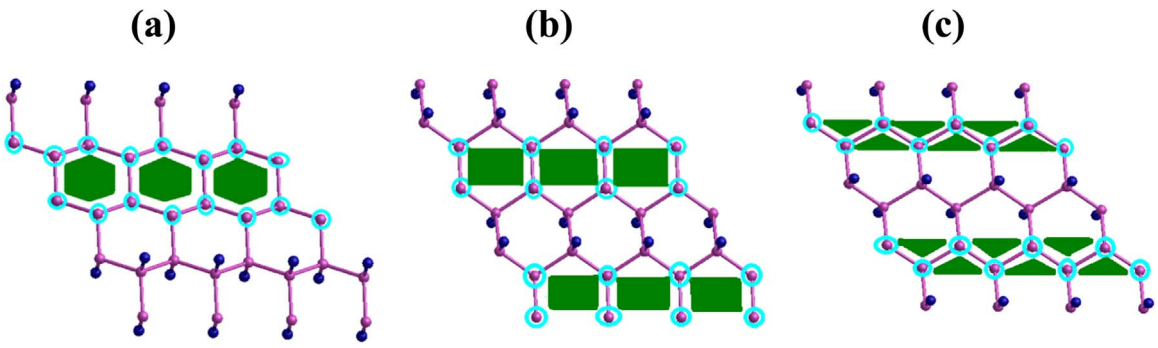

Fig. 3. Various vacancy chain patterns (a) hexagonal (b) rectangle and (c) zigzag, formed by removing alternating hexagonal, rectangle and zigzag rows respectively of X (=F, H, O) from functionalized silicene and germanene.

semiconductor. The bandgap of fluorine functionalized silicene and germanene is found to be very less as compared to the bandgap of hydrogen functionalized case which is attributed to the large electronegativity difference between F and H atoms. Semiconducting nature of X (=F, H) functionalized silicene and germanene is also revealed by the density of states (DOS) calculations (Fig. 5), where zero DOS is found in the vicinity of Fermi energy. Also, finite density of states at Fermi level, in case of O-functionalized silicene and germanene, reveals their metallic nature. It is found that in case of F- and H-functionalized silicene and germanene, the main contribution around Fermi level comes from Si or Ge atoms, while equal contribution from oxygen in the vicinity of Fermi energy in O-functionalized silicene and germanene leads to their metallic characteristics (Fig. 5). Our spin-polarized calculations show the functionalized silicene and germanene to be non-magnetic in nature.

3.1. Vacancy clusters in functionalized silicene and germanene

Now we look at the electronic and magnetic properties of functionalized silicene with created vacancy clusters (Fig. 2). It is found that, hexagonal- and rectangle-shaped vacancy clusters in SiF and GeF remain semiconducting in comparison with pentagonal- and triangle-shaped vacancy clusters. Note that hexagonal and rectangle vacancy clusters confine even number of electrons i.e. six and four respectively in the created vacancy region, those get paired-up, thereby, resulting into small change in the bandgap of SiF and GeF (Table 1) with the appearance of dispersionless or flat bands as conduction levels (Figs. 6 and S1 of Supplementary information). Whereas pentagonal and triangle vacancy clusters confine five and three electrons respectively that results into flat bands on or near the Fermi level due to odd free electron (Fig. 6) and metallicity of SiF and GeF.

Electronic band structure calculations of SiH and GeH show semiconducting nature of all the created vacancy patterns, however, with smaller bandgap value as compared to functionalized

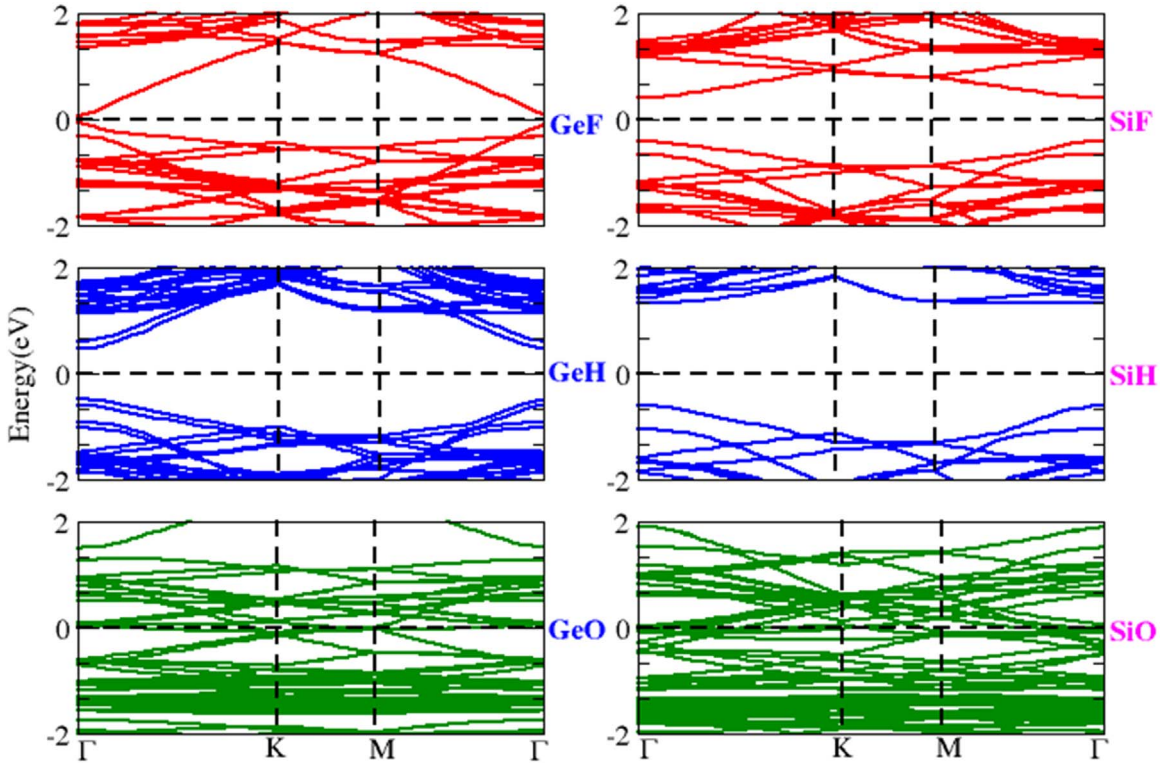

Fig. 4. Electronic band structure of X (=F, H, O) functionalized silicene and germanene. Fermi energy is set at 0 eV.

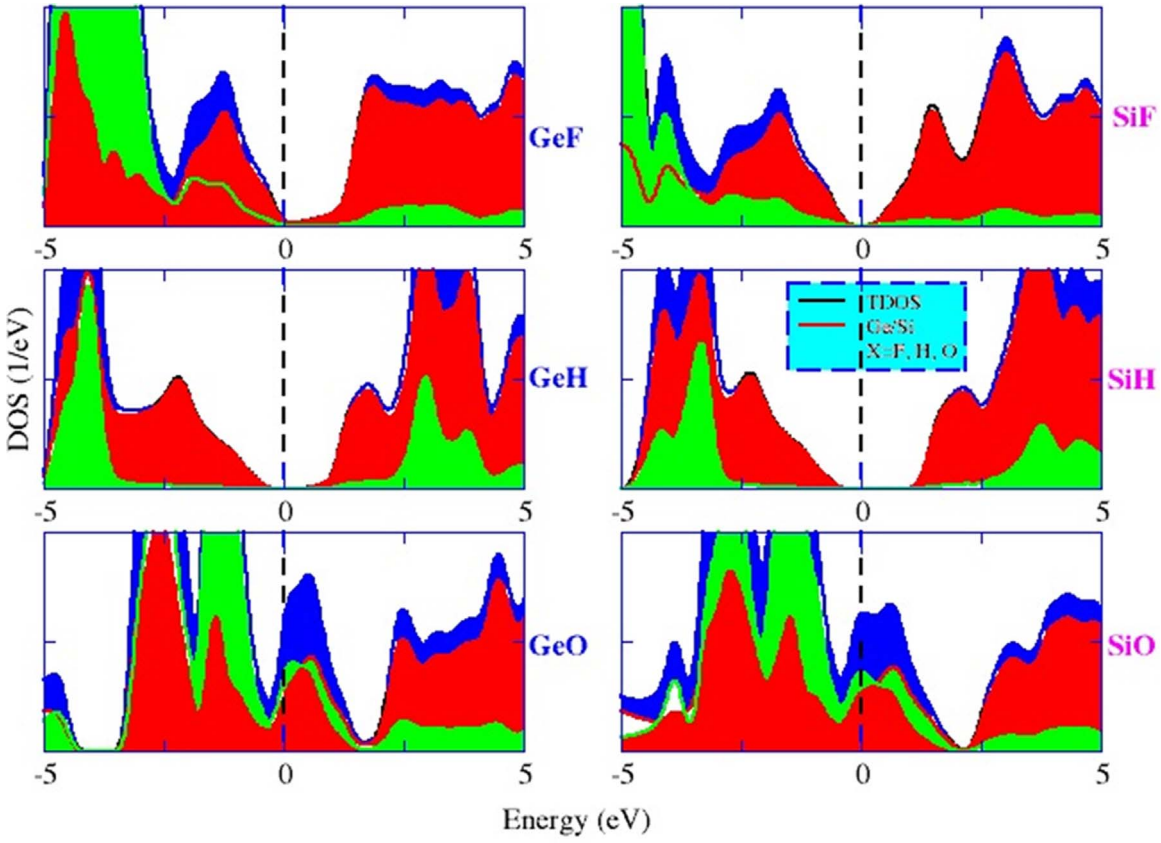

Fig. 5. Total and partial density of states (DOS) of X (=F, H, O) functionalized silicene and germanene. Fermi energy is set at 0 eV.

monolayers (Table 1). The bandgap of even confined electrons (hexagonal and rectangle) is higher than the odd confined electrons (pentagonal and triangle). Note that flat band due to confined electrons appear close to Fermi energy for odd electrons as compared to even confined ones (Figs. 6 and S1 of Supplementary information). Oxygen functionalized silicene and

Table 1
Electronic bandgap (E_g) of X (=F, H, O) functionalized silicene and germanene, with having hexagonal, pentagonal, rectangle and triangle vacancy clusters. 'M' indicate system is metallic or zero bandgap.

System	E_g (eV)				
	Functionalized	Hexagonal	Pentagonal	Rectangle	Triangle
SiF	0.81	0.99	M	0.66	M
SiH	1.92	1.00	0.58	0.98	0.93
SiO	M	M	M	M	M
GeF	0.12	0.18	M	0.19	M
GeH	0.94	0.69	0.34	0.43	0.72
GeO	M	0.093	M	M	M

germanene remains metallic after creating various vacancy clusters except hexagonal one, in which ~0.09 eV bandgap gets induced (Fig. S1 of Supplementary information for hexagonal GeO).

Our spin-polarized calculations for X (=F, H) functionalized silicene and germanene with hexagonal and rectangle vacancy cluster show zero net magnetic moment due to the even number of nearest-neighbor vacancy electrons which get paired-up. In case of pentagonal vacancy cluster in SiF/GeF and SiH/GeH, 1 μ_B net magnetic moment has been calculated which is attributed to the odd numbers of nearest-neighbor vacancies where one unpaired electron lead to total magnetic moment of 1 μ_B per unit cell. Whereas for triangle shaped vacancy cluster with three of the H/F vacancies are not adjacent to one another, that results into a total magnetic moment of 3 μ_B in the unit cell. Additionally, some fractional magnetic moment is noted for GeH (Table S1 of Supplementary information) which becomes negligible when calculated per atom. On the other hand, SiO/GeO with all the studied vacancy patterns shows zero net magnetic moment per unit cell which may be due to the pairing of the spins of vacancy electrons with the unpaired electron present on the O atom.

The evidence of magnetic/non-magnetic nature of the functionalized silicene and germanene can be seen in calculated spin-polarized DOS in Figs. 7 and S2 of Supplementary information. For example, there is significant difference between the spin up and

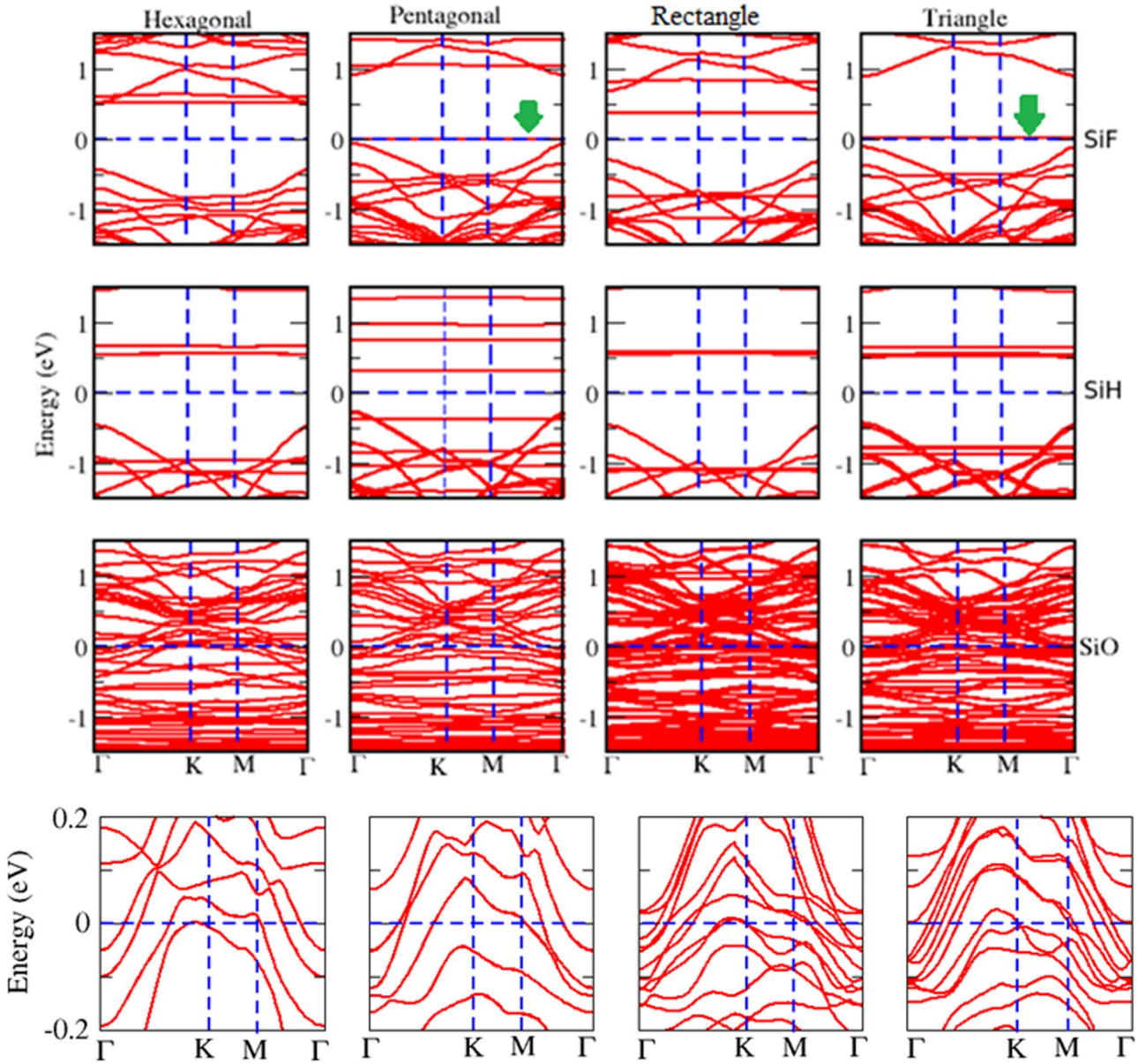

Fig. 6. Electronic band structures of X (=F, H, O) functionalized silicene having hexagonal, pentagonal, rectangle and triangle vacancy clusters. Arrow in pentagonal and triangle SiF bandstructure indicates the electronic band overlapping with Fermi level. The lowermost panel shows the enlarge view of bands around Fermi energy in SiO.

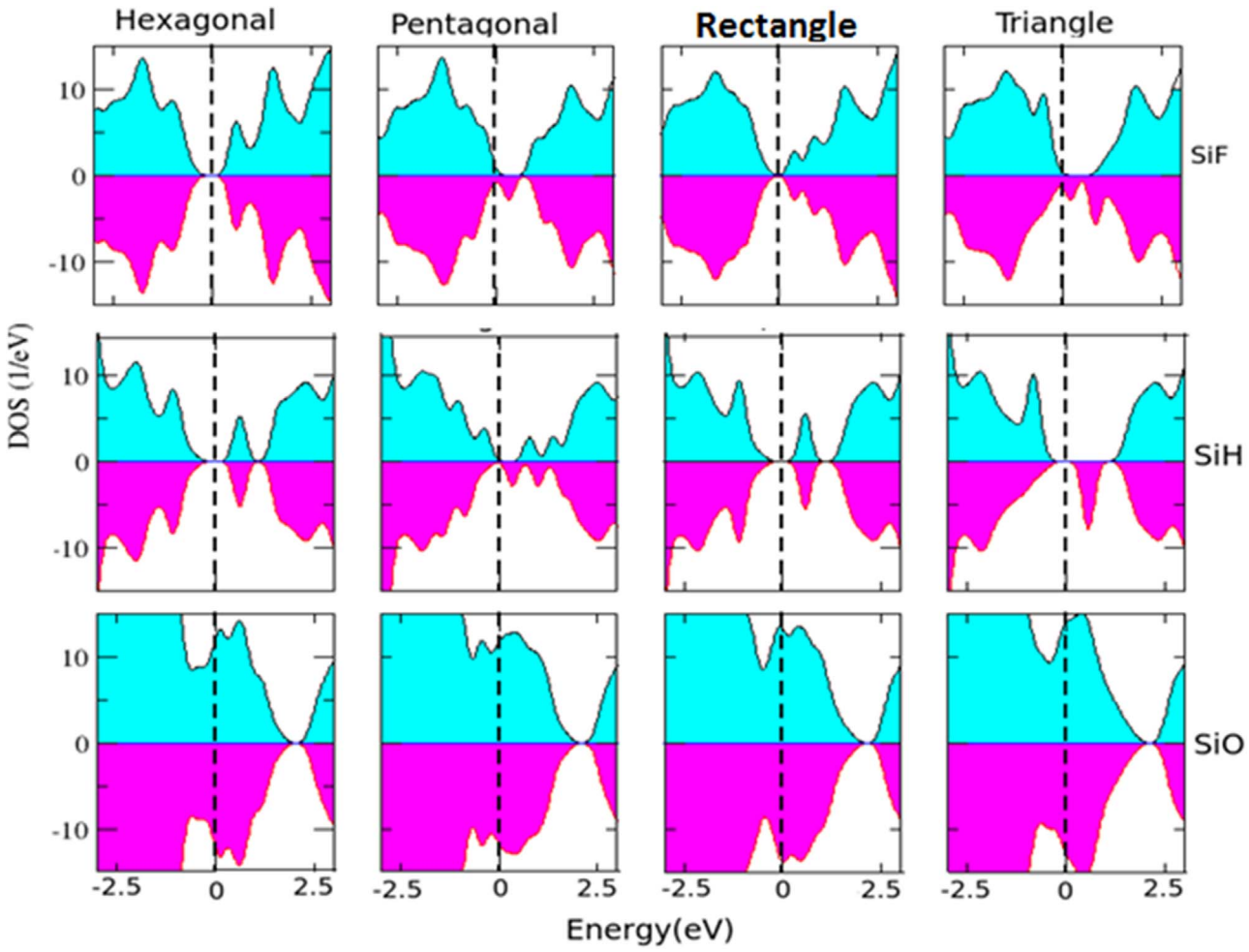

Fig. 7. Spin-polarized density of states (DOS) of X (=F, H, O) functionalized silicene having hexagonal, pentagonal, rectangle and triangle vacancy clusters.

spin down DOS of SiF having triangle vacancy cluster that leads to finite value of net magnetic moment per unit cell, while equal spinup and spin down DOS for SiF having hexagonal vacancy cluster indicates its zero net magnetic moment. Similarly, there is no difference between the spinup and spin down DOS for vacancy clusters in oxygen functionalized silicene and germanene (Figs. 7 and S2 of Supplementary information) that suggest their non-magnetic character.

3.2. Vacancy chains in functionalized silicene and germanene

Electronic band structure and DOS calculations of functionalized silicene and germanene with various vacancy chains patterns (Fig. 3) are shown in Figs. 8 and S3 and S4. The calculated bandgap values of considered functionalized silicene and germanene having vacancy chain patterns are significantly smaller than the valued obtained for functionalized monolayers with various vacancy clusters. The calculated band gap values for vacancy chain containing functionalized monolayers ranges from 0 meV to 930 meV (Table 2).

Both functionalized silicene and germanene having hexagonal chain vacancy pattern are indirect bandgap semiconductor (Figs. 8 and S3 and S4). SiF with rectangle vacancy chain and SiO, GeF and GeO with zigzag vacancy patterns show metallic characteristics, while remaining configurations are direct bandgap semiconductors. It is important to note that SiO and GeO with hexagonal and rectangle vacancy chains patterns show semiconducting nature in comparison with the metallic characteristics in fully functionalized form. The semiconducting and metallic characteristics are also evident from the calculated DOS shown in Figs. 8 and S3 and S4. It is found from our spin polarized calculations that various chain vacancies created in functionalized silicene and germanene do not induce any magnetic moment in the functionalized monolayers.

3.3. Stability and relative formation energy of functionalized silicene and germanene

It is found that the vacancy clusters and chains patterns show reconstruction of Si or Ge atoms in functionalized monolayer of silicene or germanene. For example, the Si–Si bond length (Si–Si–Si bond angle) at vacancy cluster site decreases (increases) nearly by 0.11 Å (6°), 0.13 Å (8°), 0.17 Å (5°) and 0.01 Å (3°) for hexagonal, pentagonal, rectangle and triangle vacancy clusters in fluorine functionalized silicene [Fig. S5 of Supplementary information]. Similarly, vacancy chain patterns also reconstruct the position of Si or Ge atoms as shown in Fig. S6 of Supplementary information. Note that the functionalized silicene and germanene exhibit large buckling of Si or Ge atoms as compared the corresponding pristine monolayers [Table 3]. In order to find out the energetics of various vacancy patterns, we have calculated the relative formation energy (E_f) of pristine as well as functionalized silicene and germanene. The calculated formation or cohesive energy of pristine silicene and germanene is 5.03 eV/atom and 4.25 eV/atom, respectively. The cohesive energy of functionalized silicene and germanene is listed in Table 3. Note that cohesive energy per atom of pristine

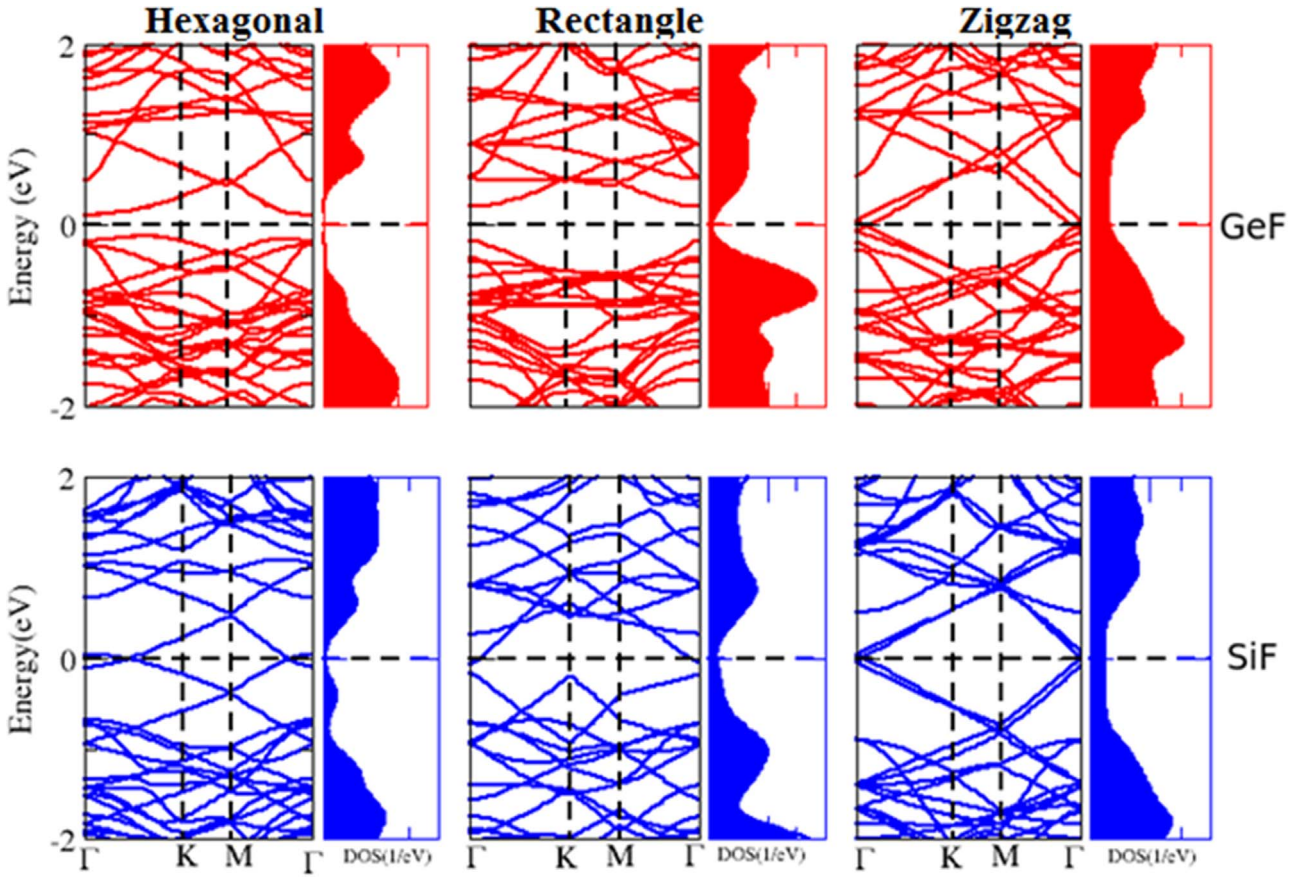

Fig. 8. Electronic band structures of fluorene-functionalized silicene and germanene having alternating hexagonal, rectangle and zigzag vacancy chains.

Table 2
Electronic bandgap (E_g) of X (=F, H, O) functionalized silicene and germanene having hexagonal, rectangle and zigzag vacancy chains at alternate position within unitcell. 'I' and 'D' represent indirect and direct bandgap.

System	E_g (meV)		
	Hexagonal	Rectangle	Zigzag
SiF	10 (I)	0	10 (D)
SiH	350 (I)	290 (I)	40 (D)
SiO	560 (I)	420 (D)	0
GeF	110 (I)	110 (D)	0
GeH	110 (I)	930 (I)	10 (D)
GeO	230 (I)	150 (I)	0

Table 3
Relative formation energy (E_f) in eV/vacancy atom of various clusters and chains patterns on functionalized silicene and germanene. Cohesive energy (E_c) and buckling parameter (Δ) of functionalized silicene and germanene are also given. Δ for pristine silicene and germanene is calculated as 0.49 Å and 0.63 Å, respectively. The calculated E_c of pristine silicene and germanene is 5.03 eV/atom and 4.25 eV/atom, respectively.

System	Δ (Å)	E_c (eV/atom)	E_f (eV/vacancy atom) vacancy clusters				E_f (eV/vacancy atom) vacancy chains		
			H	P	R	T	H	R	Z
SiF	0.71	5.53	5.63	5.71	5.69	6.04	5.47	5.91	5.83
SiH	0.74	4.77	4.29	4.22	4.34	4.73	4.06	4.07	4.03
SiO	1.21	5.75	6.85	6.89	7.00	7.22	5.01	5.89	6.37
GeF	0.69	4.63	5.15	5.25	5.28	5.65	4.75	4.90	4.79
GeH	0.83	4.23	3.83	3.77	3.95	4.13	3.71	3.90	3.78
GeO	1.23	5.03	5.90	6.00	6.12	6.46	4.23	4.50	5.50

monolayer is calculated as:

$$E_c = \left[E_{\text{total}} - E_{1\ (\text{Si or Ge})} - E_{2\ (\text{F or H or O})}\right]/N$$

where E_{total} is the total energy of 2D Si or Ge monolayer, E_1 and E_2 are the total energy of constituents free atoms and N is the number of atoms. It is found that the relative ease of the formation of hydrogenated silicene and germanene is energetically most favorable.

The relative formation energy of various vacancy clusters and chain patterns are calculated between 3.7 and 7.0 eV/atom [Table 3], which is obtain using the expression:

$$E_f = \left[E_{\text{total}}(\text{functionalized} + \text{vacancy}) + E_{\text{total}}(\text{vacancy}) - E_{\text{total}}(\text{functionalized})\right]/N_v$$

where E_{total} (functionalized + vacancy) is the total energy of functionalized monolayer with vacancy clusters and chain, E_{total} (vacancy) is total energy of N_v free vacancy atoms, E_{total} (functionalized) is the total energy of fully functionalized layer of silicene or germanene. It is found that the vacancy clusters and chains patterns formed on hydrogenated silicene and germanene are energetically most stable. Note that the formation energy has been found to show strong dependence on the size of vacancy clusters, which decreases with the increase in size of vacancy patterns [35].

3.4. STM topographical images

It was previously found that STM topographical images can be used as electronic fingerprints to identify DNA nucleotide bases on graphene, which provide alternative route to the DNA sequencing using scanning tunneling spectroscopy [36]. Also it is well established that STM images can be simulated using DFT by applying

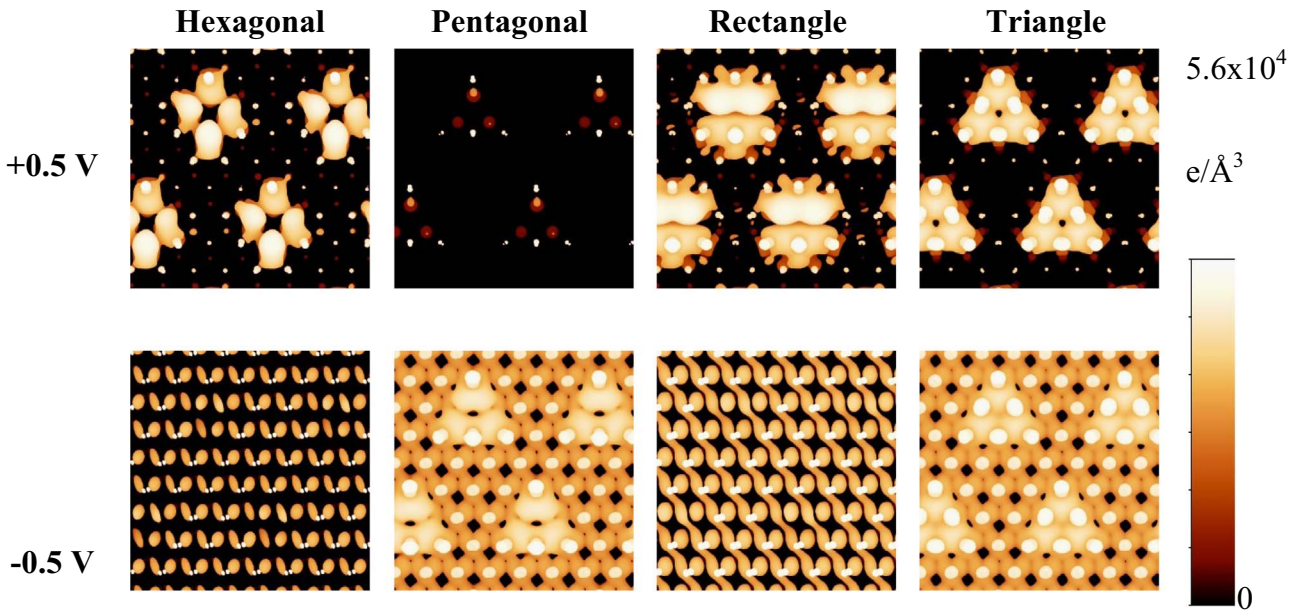

Fig. 9. Simulated STM topographical images of a 30 Å × 30 Å area of fluorene-functionalized silicene having hexagonal, pentagonal, rectangle and triangle vacancy clusters at ± 0.5 V bias voltage.

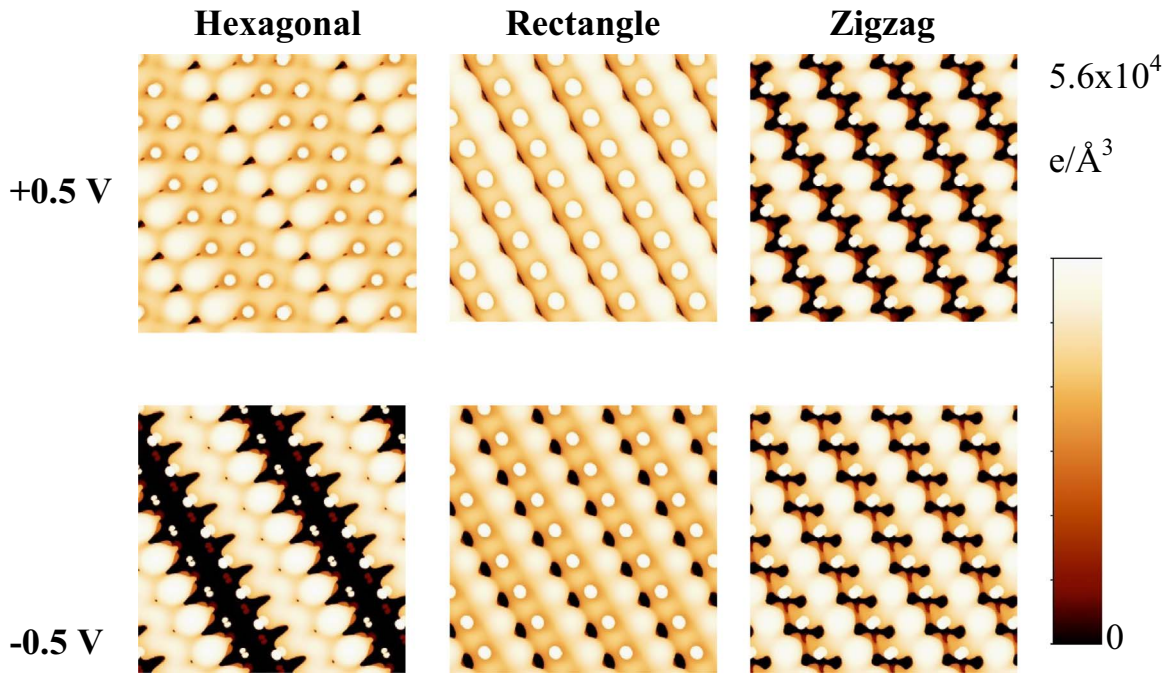

Fig. 10. Simulated STM topographical images of a 30 Å × 30 Å area of fluorene-functionalized silicene having hexagonal, rectangle and zigzag vacancy chains at ± 0.5 V bias voltage.

the small bias voltage (V_{bias}) between the sample and STM tip that yields tunneling current which can further be approximated within Tersoff and Hamann approximation [37]. In this approximation, tunneling current (I) is proportional to the local density of states (LDOS) integrated from ($E_F - eV_{bias}$) to E_F and the tip states are described by s-waves with constant density of states. Within this framework, a positive (negative) bias provides information about the electron density corresponding to the occupied (unoccupied) states.

In our calculations, STM images have been obtained in constant current (CC) mode and derived from LDOS using WSxM code [38]. The tip-sample distance is defined as the distance between the atomic planes and the point-like tip, by considering the fact that neither tip shape nor its electronic structure are taken into account in our calculations. As a case study, we present here the STM calculations of SiF with various vacancy clusters and chain patterns. Note that there are significantly different features in DOS (Figs. 7 and S2–S4) as far as the states near the Fermi energy are concerned. Therefore, these features can be served as an electronic fingerprints for experimental STM.

The calculated STM images for considered vacancy clusters and vacancy chain patterns at ± 0.5 V bias are shown in Figs. 9 and 10 respectively. The difference in the brightness of images between the sign of the bias voltage is directly related to the localized states in the corresponding DOS, which could be an important aspect to interpret the corresponding experimental images. It is noteworthy

that different vacancy patterns show significantly different images (Figs. 9 and 10), which can used as electronic fingerprints for experimental STM for the identifications of various vacancies introduced in the process of functionalization.

4. Conclusions

In summary, first principles calculations are performed to see the effect of various vacancy clusters and chain patterns of F-, H- and O-functionalized silicene and germanene. Hexagonal and rectangle vacancy clusters in F-functionalized silicene and germanene modify the electronic bandgap of monolayer with retention of semiconducting nature while pentagonal and triangle vacancy clusters introduce metallicity in the monolayers. H-functionalized monolayers having all types of vacancy clusters show semiconducting characteristics with modified bandgap values. Also pentagonal and triangle vacancy clusters induce 1 μ_B and 3 μ_B magnetic moment respectively in monolayer. O-functionalized silicene and germanene remains metallic and non-magnetic after creating various vacancy patterns except hexagonal vacancy cluster where ~90 meV gap get induced. Bandgap also gets induced in otherwise metallic SiO and GeO on creating hexagonal and rectangle vacancy chain patterns. Our calculated STM topographical images show distinctly different characteristics for various vacancy clusters and chain patterns which may be used as electronic fingerprints to guide the experimentalist in order to identify various vacancy patterns in silicene and germanene during the process of functionalization.

Acknowledgments

We gratefully acknowledge SIESTA team for code. PJ is grateful to UGC-BSR for financial assistance in the form of Junior Research Fellowship. MS acknowledge DST for financial assistance in the form of INSPIRE fellowship. CVRAMAN, HPCC at Himachal Pradesh University has been used for obtaining most of the results presented in the paper, while Rama, a high performance computing cluster, at Michigan Technological University, is partially used to obtain some results.

Appendix A. Supplementary material

Supplementary data associated with this article can be found in the online version at http://dx.doi.org/10.1016/j.physe.2016.08.015.

References

[1] S.Z. Butler, S.M. Hollen, L. Cao, Y. Cui, J.A. Gupta, H.R. Gutierrez, T.F. Heinz, S. S. Hong, J. Huang, A.F. Ismach, et al., Progress, challenges, and opportunities in two-dimensional materials beyond graphene, ACS Nano 7 (2007) 2898–2926.
[2] A. Dimoulas, Silicene and germanene: silicon and germanium in flat land, Microelectron. Eng. 131 (2015) 68–78.
[3] R. Stephan, E. Motohiko, Giant magneto-resistance and perfect spin filter in silicene, germanene and stanene, Phys. Rev. B 89 (2014) 195303.
[4] T.P. Kaloni, U. Schwingenschlogl, Weak interaction between germanene and GaAs(0001) by H intercalation: a route to exfoliation, J. Appl. Phys. 114 (2013) 184307.
[5] Z.Y. Ni, Q.H. Liu, K.C. Tang, J.X. Zheng, J. Zhou, R. Qin, Z.X. Gao, D.P. Yu, J. Lu, Tunable bandgap in silicene and germanene, Nano Lett. 12 (2012) 113–118.
[6] N.J. Roome, J.D. Carey, Beyond graphene: stable elemental monolayer of silicene and germanene, ACS Appl. Mater. Interfaces 6 (2014) 7743–7750.
[7] B. Mohan, A. Kumar, P.K. Ahluwalia, A first principle calculation of electronic and dielectric properties of electrically gated low-buckled mono and bilayer silicene, Physica E 53 (2013) 233–239.
[8] S. Cahangirov, M. Topsakal, E. Aktrk, H. Sahin, S. Ciraci, Two- and one-dimensional honeycomb structures of silicon and germanium, Phys. Rev. Lett. 102 (2009) 236804.
[9] P. Vogt, P. De Padova, C. Quaresima, J. Avila, E. Frantzeskakis, M.C. Asensio, A. Resta, B. Ealet, G. Le Lay, Silicene: compelling experiment evidence for graphene like two-dimensional silicon, Phys. Rev. Lett. 108 (2012) 155501.
[10] B. Feng, Z. Ding, S. Meng, Y. Yao, X. He, P. Cheng, L. Chen, K. Wu, Evidence of silicene in honeycomb structure of silicon on Ag(111), Nano Lett. 12 (2012) 3507–3511.
[11] L. Chen, C.C. Liu, B. Feng, X. He, P. Cheng, Z. Ding, S. Meng, Y. Yao, K. Wu, Evidence for Dirac fermions in a honeycomb lattice based on silicon, Phys. Rev. Lett. 109 (2012) 056804.
[12] M.E. Devlla, L. Xian, S. Cahang Irov, A. Rublo, G. Le Lay, Germanene: a novel two-dimensional germanium akin to graphene and silicene, New J. Phys. 16 (2014) 095002.
[13] L. Meng, Y. Wang, L. Zhang, S. Du, R. Wu, L. Li, Y. Zhang, G. Li, H. Zhou, W. A. Hofer, H.J. Gao, Buckled silicene formation on Ir(111), Nano Lett. 13 (2013) 685–690.
[14] A.K. Singh, E.S. Penev, B.I. Yakobson, Vacancy cluster in graphene as quantum dots, ACS Nano 4 (2010) 3510–3514.
[15] P. Jamdagni, A. Kumar, R. Pandey, A. Takur, P.K. Alhuwalia, Stability and electronic properties of SiGe based 2D layered structures, Mater. Res. Express 2 (2015) 016301.
[16] Y. Li, Z. Chen, Tuning electronic properties of germanane layers by external electric field and biaxial tensile strain: a computational study, J. Phys. Chem. C 118 (2014) 1148–1154.
[17] P. Jamdagni, A. Kumar, M. Sharma, A. Thakur, P.K. Ahluwalia, Electronic, mechanical and dielectric properties of silicane under tensile strain, AIP Conf. Proc. 1661 (2015) 080007.
[18] A. Atsalakis, L. Tsetseris, First-principles study of siloxene and germoxene: stable conformation, electronic properties, and defects, J. Phys.: Condens. Matter 26 (2014) 285301.
[19] Y. Wang, J. Zheng, Z. Ni, R. Fei, Q. Liu, R. Quhe, C. Xu, J. Zhou, Z. Gao, J. Lu, Half-metallic silicene and germanene nanoribbons: towards high-performance spintronics device, Nano 7 (2012) 1250037.
[20] P. Jamdagni, A. Kumar, M. Sharma, A. Thakur, P.K. Ahluwalia, Electronic and mechanical properties of hybrid graphene/h-BN nanoribbons, AIP Conf. Proc. 1665 (2015) 090023.
[21] D.C. Elias, R.R. Nair, T.M.G. Mohiuddin, S.V. Morozov, P. Blake, M.P. Hallsall, A. C. Ferrari, D.W. Boukhvalov, M.I. Katsnelson, A.K. Geim, K.S. Novoselov, Control of graphene's properties by reversible hydrogenation: evidence for graphene, Science 323 (2009) 610–613.
[22] R.R. Nair, W. Ren, R. Jalil, I. Riaz, V.G. Kravets, L. Britnell, P. Blake, F. Schedin, A. S. Mayorov, S. Yuan, M.I. Katsnelson, H.M. Cheng, W. Strupinski, L. G. Bulusheva, A.V. Okotrub, I.V. Grigorieva, A.N. Grigorenko, K.S. Novoselov, A. K. Geim, Fluorinated graphene: fluorographene: a two-dimensional counterpart of Teflon, Small 6 (2010) 2773.
[23] N. Gao, W.T. Zheng, Q. Jiang, Density functional theory calculations for two-dimensional silicene with halogen functionalization, Phys. Chem. Chem. Phys. 14 (2012) 257–261.
[24] C. Si, J. Liu, Y. Xu, J. Wu, B.L. Gu, W. Duan, Functionalized germanene as a prototype of large-gap two-dimensional topological insulators, Phys. Rev. B 89 (2014) 115429.
[25] R. Wang, X. Pi, Z. Ni, Y. Liu, S. Lin, M. Xu, D. Yang, Silicene oxides: formation, structures and electronics properties, Sci. Rep. 3 (2013) 3507.
[26] G. Liu, S.B. Liu, B. Xu, C.Y. Ouyang, L.X. Li, H.Y. Song, The stability of free standing germanene in oxygen: first-principles investigation, Europhys. Lett. 110 (2015) 17007.
[27] Y. Wang, Yc Ding, Mechanical and electronic properties of stoichiometric silicene and germanene oxides from first-principles, Phys. Status Solidi RRL 7 (6) (2013) 410–413.
[28] Jinglan Qiu, Huixia Fu, Yand Xu, A.I. Oreshkin, Tingna Shao, Hui Li, Sheng Meng, Lan Chen, Kehui Wu, Ordered and reversible hydrogenation of silicene, Phys. Rev. Lett. 114 (2015) 126101.
[29] Jinglan Qiu, Huixia Fu, Yang Xu, Qing Zhou, Sheng Meng, Hui Li, Lan Chen, Kehui Wu, From silicene to half-silicane by hydrogenation, ACS Nano 9 (2015) 11192–11199.
[30] Arnab Majumdar, Suman Chowdhury, Palash Nath, Debnarayan Jana, Defect induced magnetism in planar silicene: a first principles study, RSC Adv. 4 (2014) 32221–32227.
[31] H. Sahin, C. Ataca, S. Ciraci, Magnetization of graphene by dehydrogenation, Appl. Phys. Lett. 95 (2009) 222510.
[32] J. Berashevich, T. Chakraborty, Sustained ferromagnetic induced by H-vacancies in graphene, Nanotechnology 21 (2010) 355201.
[33] J.M. Soler, E. Artacho, J.D. Gale, A. García, J. Junquera, P. Ordejon, l D.S. Porta, The SIESTA method for ab-initio order-N materials simulation, J. Phys. Condens. Matter 14 (2002) 2745.
[34] N. Troullier, J.L. Martins, Efficient pseudopotentials for plane-wave calculation. II. Operators for fast iterative diagonalisation, Phys. Rev. B 43 (1991) 8861.
[35] B.-Ru Wu, C.-Kai Yang, Electronic structures of clusters of hydrogen vacancies on graphene, Sci. Rep. 5 (2015) 15310.
[36] T. Ahmed, S. Kilina, T. Das, J.T. Haraldsen, J.J. Rehr, A.V. Balatsky, Electronic fingerprints of DNA bases on graphene, Nano Lett. 12 (2011) 927–931.
[37] J. Tersoff, D.R. Hamann, Theory of the scanning tunneling microscope, Phys. Rev. B 31 (2) (1985) 805–813.
[38] I. Horcas, R. Fernandez, J.M. Gomez-Rodriguez, J. Colchero, J. Gomez-Herrero, A.M. Baro, WSXM: a software for scanning probe microscopy and a tool for nanotechnology, Rev. Sci. Instrum. 1 (2007) 7.